

MODELLING OF NONLINEAR INDUCTOR EXHIBITING HYSTERESIS LOOPS  
AND ITS APPLICATION TO THE SINGLE PHASE PARALLEL INVERTERS

Y. Saito, H. Saotome, S. Hayano and T. Yamamura

**Abstract** - A modelling of magnetodynamic fields taking into account dynamic hysteresis loops was previously proposed for predicting three-dimensional magnetodynamic fields in electromagnetic devices [1]. This method is now applied to construct the lumped circuit model for nonlinear inductor exhibiting dynamic hysteresis loops. The lumped circuit model of nonlinear inductor is introduced into the simulation model of single phase parallel inverter, whose various characteristics are calculated and compared with experimental measurements. Good agreement is obtained.

INTRODUCTION

Depending upon the circumstances, it may be sufficient to assume that the hysteresis loss can be represented in terms of a resistance loss. However it is most difficult to construct a model having the accuracy for analysis of nonlinear circuits such as ferroresonant circuit [2]. Chua and Stromsroe worked out the hysteresis model for electronic circuit studies [3]. Also, Talukdar and Bailey worked out the hysteresis model for power system studies [4].

In this paper, the Saito, Saotome and Yamamura model of nonlinear inductor is generalized to include the transformers, and applied to the simulation of single phase parallel inverter.

MODELLING OF NONLINEAR INDUCTOR

The magnetic field equation exhibiting dynamic hysteresis loops is given by

$$H = \left(\frac{1}{\mu}\right)B + \left(\frac{1}{s}\right)\frac{dB}{dt} \tag{1}$$

where  $H, B, \mu, s$  and  $t$  denote the magnetic field intensity, flux density, permeability, hysteresis coefficient and time, respectively. The term  $(1/\mu)B$  in (1) represents the magnetic saturation property of iron and the other term  $(1/s)dB/dt$  represents the dynamic hysteresis property of iron. Moreover a trace of the peak points on the hysteresis loops yields a single valued function of permeability  $\mu$  as shown in the left-hand curve of Fig. 1. Also, a trace of the peak points on the loops representing the relation between the magnetic field intensity  $H$  and time derivative of flux density  $dB/dt$  yields another single valued function of hysteresis coefficient  $s$  as shown in the right-hand curve of Fig. 1 [1,2].

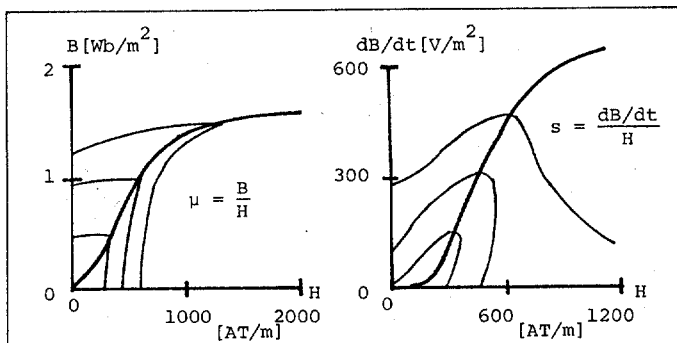


Fig. 1. Nonlinear magnetization curves.

The authors are with College of Engineering, Hosei University, 3-7-2 Kajinocho Koganei, Tokyo 184, Japan.

The hysteresis phenomenon is inevitably observed accompanying with the time derivative of flux density  $dB/dt$ . When the magnetic field intensity  $H$  in (1) is gradually reduced to zero, then the right-hand term  $(1/\mu)B + (1/s)dB/dt$  in (1) must be reduced to zero. By considering an infinitesimally small  $dB/dt$  point on the trace of peak points representing the relation  $dB/dt$  and  $H$  in Fig. 1, the magnetic field intensity  $H_s = (1/s)dB/dt$  tends to keep a non-zero value. Thereby, the term  $(1/\mu)B$  or  $B$  in (1) must take a non-zero value when the term  $dB/dt$  in (1) is an infinitesimally small value. This means that (1) is possible to exhibit the static magnetic hysteresis phenomenon.

Since the magnetic hysteresis phenomenon is always observed accompanying with the time derivative of flux density  $dB/dt$ , the magnetization history is implicitly included in the formula (1) as an initial value of  $B$ .

When the time derivative of flux density  $dB/dt$  takes the same absolute value, then the term  $H_s = (1/s)dB/dt$  in (1) takes the same absolute values for descending and ascending branches of the hysteresis loops. However, the time derivative of flux density  $dB/dt$  takes a negative value for descending and an positive value for ascending branches of the hysteresis loops. Thereby, the total magnetic field intensity  $H$  in (1) reduces to  $H = (1/\mu)B - (1/s)dB/dt$  for descending and to  $H = (1/\mu)B + (1/s)dB/dt$  for ascending branches of the positive flux density ( $B > 0$ ) regions in hysteresis loops. This means that the magnetic flux density  $B$  corresponds to the different magnetic field intensities for descending and ascending branches of the hysteresis loops.

Thus, the formula (1) is possible to reproduce the hysteresis phenomenon which is consistent with the experimental results.

In order to derive the lumped circuit model of nonlinear inductor, consider a simple reactor as shown in Fig. 2(a). By considering (1) and Fig. 2(a), it is possible to write the following equation as

$$\int_0^D H dl = \int_0^D \left[ \left(\frac{1}{\mu}\right)B + \left(\frac{1}{s}\right)\frac{dB}{dt} \right] dl, \tag{2}$$

where  $D$  and  $dl$  denote the mean length of flux path and infinitesimally small distance along the flux path  $D$ , respectively. With  $A$  denoting the cross-sectional area normal to the flux path, the relationship between the flux density  $B$  and flux  $\phi$  is given by  $B = \phi/A$ . Thus, the right-hand term in (2) can be rewritten by

$$\int_0^D \left[ \left(\frac{1}{\mu}\right)B + \left(\frac{1}{s}\right)\frac{dB}{dt} \right] dl = \frac{1}{L_i} \phi + \frac{1}{R_i} \frac{d\phi}{dt}, \tag{3}$$

where the inductance  $L_i$  and resistance  $R_i$  are defined by  $L_i = \mu A/D$  and  $R_i = sA/D$ , respectively. Moreover, the

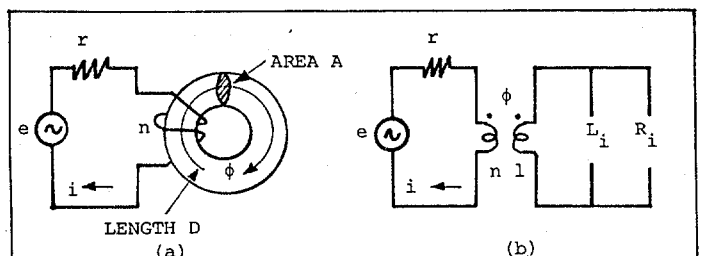


Fig. 2. (a) Schematic diagram of nonlinear inductor and (b) its circuit model.

left-hand term in (2) can be represented in terms of the impressed voltage  $e$ , current  $i$ , electric resistance  $r$ , flux  $\phi$  and number of turns of coil  $n$ , that is

$$\int_0^D H dl = ni = \frac{n}{r} [e - n \frac{d\phi}{dt}] \quad (4)$$

By substituting (3), (4) into (2), it is possible to write the following relation:

$$ni = \frac{n}{r} [e - n \frac{d\phi}{dt}] = \frac{1}{L_i} \phi + \frac{1}{R_i} \frac{d\phi}{dt} \quad (5)$$

By means of (5), it is possible to derive the lumped circuit model of nonlinear inductor as shown in Fig. 2(b), where the transformer shown is an ideal transformer. As shown in Fig. 1, the permeability  $\mu$  and hysteresis coefficient  $s$  are respectively the functions of the flux density  $B$  and the time derivative of flux density  $dB/dt$ . Furthermore, the relationship between the flux density  $B$  and flux  $\phi$  is given by  $B = \phi / (\text{Cross-Sectional Area Normal to the Flux Path})$ , therefore the inductance  $L_i$  and resistance  $R_i$  in (5) are formally expressed as

$$L_i = f_{\mu}(\phi), \quad (6)$$

$$R_i = f_s(d\phi/dt), \quad (7)$$

where  $f(*)$  denotes the single valued function of  $(*)$ .

If a new set of variables  $\lambda = n\phi$ ,  $L = n^2 L_i$ ,  $R = n^2 R_i$  is substituted into (5), then the lumped circuit model of nonlinear inductor reduces to the previous one [2].

APPLICATION TO THE SINGLE PHASE PARALLEL INVERTER

As a practical application of our lumped circuit model for the nonlinear inductor, we applied our nonlinear inductor model to the single phase parallel inverter.

Figure 3(a) shows the schematic diagram of single phase parallel inverter. Also, Fig. 3(b) shows the circuit model of single phase parallel inverter. The system of circuit equations is best expressed in matrix notation involving the voltage vector  $V$ , current vector  $I$ , conductance matrix  $G$ , winding matrix  $N$  and flux vector  $\phi$ , viz.,

$$I = G[V - N(d/dt)\phi], \quad (8)$$

where

$$V = [E, E, 0]^T, \quad (9)$$

$$I = [i_a, i_b, i_c]^T, \quad (10)$$

$$\phi = [\phi_d, \phi, q]^T, \quad (11)$$

$$G = \begin{bmatrix} r_d + r_a + r_{as} & r_d & 0 \\ r_d & r_d + r_b + r_{bs} & 0 \\ 0 & 0 & r_c \end{bmatrix}^{-1}, \quad (12)$$

$$N = \begin{bmatrix} n_d & n_a & r_{as} \\ n_d & -n_b & -r_{bs} \\ 0 & n_c & 0 \end{bmatrix}. \quad (13)$$

The elements  $E, i_a, i_b, i_c, \phi_d, \phi, q, r_a, r_b, r_c, r_d, n_a, n_b, n_c, n_d$  in (9)-(13) are shown in Fig. 3; and the superscripts  $T, -1$  in (9)-(12) denote the transpose and inverse of matrix, respectively. The resistances of SCR (Silicon Controlled Rectifier) are denoted by  $r_{as}, r_{bs}$  as shown in Fig. 3.

On the other side, the current vector  $I$  in (8) must be related to the flux vector  $\phi$  by

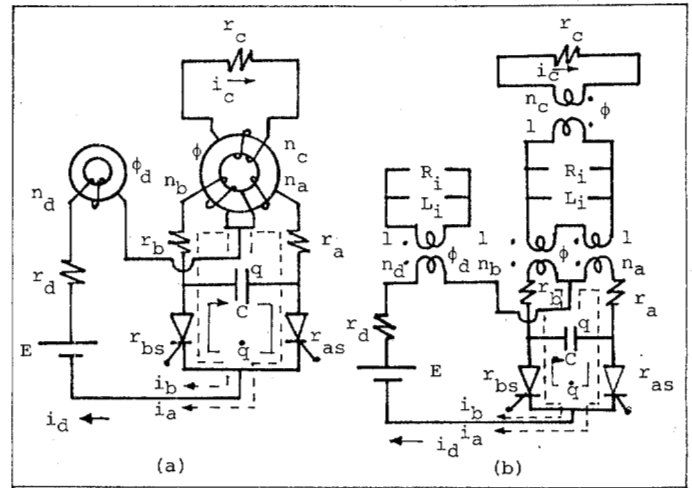


Fig. 3. (a) Schematic diagram of single phase parallel inverter and (b) its circuit model.

$$N^T I = M\phi + H(d/dt)\phi, \quad (14)$$

where

$$M = \begin{bmatrix} 1/L_i & 0 \\ 0 & 1/L_i & 0 \\ 0 & 0 & -1/C \end{bmatrix}, \quad (15)$$

$$H = \begin{bmatrix} 1/R_i & 0 & 0 \\ 0 & 1/R_i & 0 \\ 0 & 0 & -r_{as} - r_{bs} \end{bmatrix}. \quad (16)$$

The inductance  $L_i$  in (15) and resistance  $R_i$  in (16) are shown in Fig. 2(b); and the inverting capacitor  $C$  in (15) is shown in Fig. 3. By substituting (8) into (14) and rearranging, the system of circuit equations which must be solved for the flux vector  $\phi$  is given by

$$(d/dt)\phi = [H + N^T GN]^{-1} [-M\phi + N^T GV]. \quad (17)$$

NUMERICAL METHOD OF SOLUTION

As shown in (6), (7), the inductance  $L_i$  and resistance  $R_i$  in (15), (16) are respectively the functions of flux  $\phi$  and the time derivative of flux  $d\phi/dt$ . Moreover, the resistances  $r_{as}, r_{bs}$  of SCR in (12), (13), (16) are the function of their terminal voltage as well as gate trigger pulse current. The forward voltage - current characteristic of SCR is similar to those of the diode when the gate trigger pulse current  $i_g$  takes a reasonable value. Thereby, it is assumed that the forward resistance of SCR may be approximately calculated by

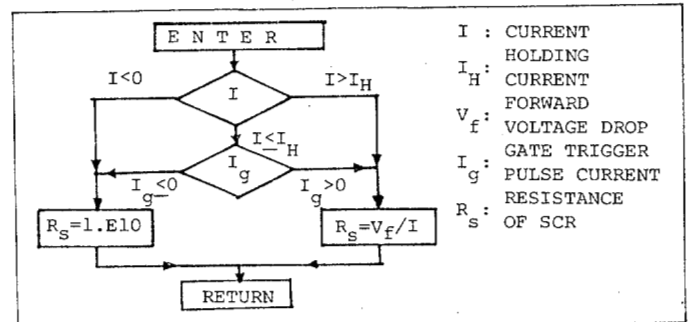


Fig. 4. Flow chart of the SCR FUNCTION.

a simple hyperbola. Also, the backward resistance of SCR is assumed to a quite large value. Figure 4 shows the flow chart of the SCR FUNCTION. Since the terminal voltage of SCR depends on the the time derivative of the flux vector  $(d/dt)\phi$ , (17) may be represented by

$$(d/dt)\phi = F[\phi, (d/dt)\phi, i_g]. \quad (18)$$

(18) means that the circuit model of single phase parallel inverter gives a system of nonlinear differential equations whose coefficients are the functions of the flux vector  $\phi$ , time derivative of flux vector  $(d/dt)\phi$  and gate trigger pulse current  $i_g$ .

For numerically solving (18), this system of nonlinear differential equations is replaced by the following divided differences:

$$\left(\frac{1}{\Delta t}\right)(\phi_{t+\Delta t} - \phi_t) = F\left[\left(\frac{1}{2}\right)(\phi_{t+\Delta t} + \phi_t), \left(\frac{1}{\Delta t}\right)(\phi_{t+\Delta t} - \phi_t), i_g\right], \quad (19)$$

where  $\Delta t$  denotes the stepwidth in time  $t$ ; subscripts  $t+\Delta t, t$  refer to the time  $t+\Delta t$  and  $t$ , respectively. With the superscripts  $(K+1), (K), (K-1)$  denoting the number of iterations, (19) is iteratively solved by

$$\phi_{t+\Delta t}^{(K+1)} = \phi_t + \Delta t F\left[\left(\frac{1}{2}\right)(\phi_{t+\Delta t}^{(K)} + \phi_t), \left(\frac{1}{\Delta t}\right)(\phi_{t+\Delta t}^{(K)} - \phi_t), i_g\right], \quad (20)$$

where  $\phi_{t+\Delta t}^{(K)}$  is

$$\phi_{t+\Delta t}^{(K)} = \phi_{t+\Delta t}^{(K-1)} + \left(\frac{1}{2}\right)[\phi_{t+\Delta t}^{(K)} - \phi_{t+\Delta t}^{(K-1)}]. \quad (21)$$

#### NUMERICAL SOLUTIONS

Various constants used in the calculations of the single phase parallel inverter shown in Fig. 3 are listed in Table 1.

Table 1. VARIOUS CONSTANTS USED IN THE CALCULATIONS.

Number of turns of DC coil	$n_d$	600 [turns]
Number of turns of primary coil (a)	$n_a^a$	300 [turns]
Number of turns of primary coil (b)	$n_a^b$	300 [turns]
Number of turns of secondary coil	$n_c$	300 [turns]
Electric resistance of DC coil	$r_d$	3.151 [ $\Omega$ ]
Electric resistance of coil (a)	$r_a^a$	1.356 [ $\Omega$ ]
Electric resistance of coil (b)	$r_a^b$	1.323 [ $\Omega$ ]
Electric resistance of secondary	$r_c$	101.84 [ $\Omega$ ]
Forward voltage drop of SCR	$V_f$	1.6 [V]
Holding current of SCR	$I_H$	0.06 [A]
DC impressed voltage	$E^H$	20 [V]

The magnetization curves used in the calculations are shown in Fig. 1, and represented by linear interpolation in the calculations. The stepwidth  $\Delta t$  in (20) was determined as  $\Delta t < 0.25$  (msec) when the convergence and accuracy of the solutions were taken into account.

Figure 5 shows the transient transformer flux  $\phi$  and the charge  $q$  on the inverting capacitor C under the

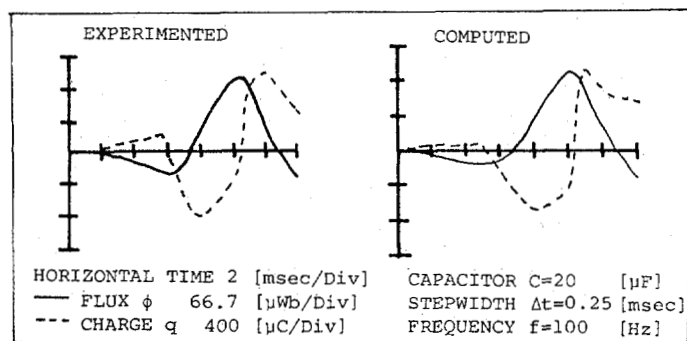


Fig. 5. Transient flux and charge under the normal operation.

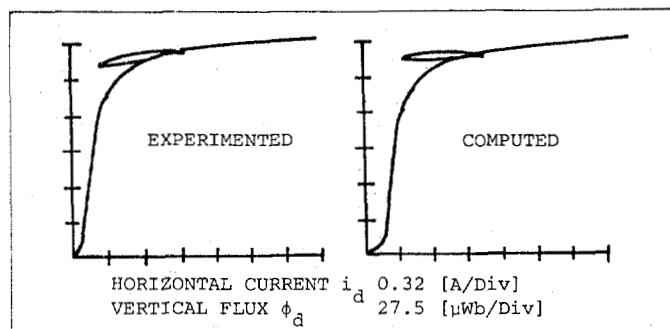


Fig. 6. Dynamic hysteresis loops under the normal operation.

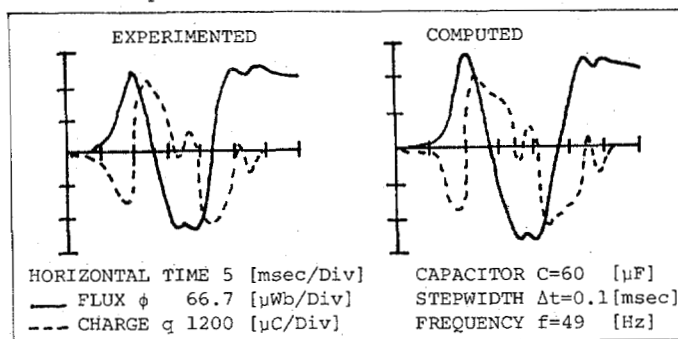


Fig. 7. Transient flux and charge under the abnormal operation.

normal operation. Also, Fig. 6 shows the dynamic hysteresis loops between the direct current  $i_d$  and the reactor flux  $\phi_d$  under the same conditions of Fig. 5.

Moreover, Fig. 7 shows the transient transformer flux  $\phi$  and the charge  $q$  on the inverting capacitor C under the abnormal operation.

By considering the results of Figs. 5-7, it is revealed that the circuit model of single phase parallel inverter in cooperation with our nonlinear inductor model behaves just look like a practical one including the abnormal operation.

#### CONCLUSION

As shown above, we have derived one of the determining nonlinear inductor model and demonstrated its applicability to the single phase parallel inverter circuit. Particularly, our approach has enabled to simulate the SCR circuits without considering the switching problem of SCR.

The time required to obtain the results of Fig. 5 was about 5 minutes on the computer ACOS-6/SYSTEM 700 at the Computer Center of Hosei University.

#### REFERENCES

- [1] Y.Saito, "Three-Dimensional Analysis of Magnetodynamic Fields in Electromagnetic Devices taken into account the Dynamic Hysteresis Loops," *IEEE Transaction on Magnetics*, Vol. MAG-18, No. 2, March 1982, pp. 546-551.
- [2] Y.Saito, H.Saotome and T.Yamamura, "A Lumped Circuit Model for Nonlinear Inductor Exhibiting Dynamic Hysteresis Loops and its Application to the Electric Circuits," *Comp. Meths. Appl. Mech. Eng.*, to be published.
- [3] L.O.Chua and K.A.Stromsmoe, "Lumped Circuit Models for Nonlinear Inductor Exhibiting Hysteresis Loops," *IEEE Transaction Circuit Theory*, Vol. CT-17, No. 4, Nov. 1970, pp. 564-574.
- [4] S.N.Talukdar and J.R.Bailey, "Hysteresis Model for System Studies," *IEEE Transaction Power Apparatus and Systems*, Vol. PAS-95, No. 4, July 1976, pp. 1429-1432.